

# Control and Tracking of Unstable Orbits in Hamiltonian Flows: The Diamagnetic Kepler Problem

Babak Pourbohloul and Louis J. Dubé\*

*Département de Physique, Université Laval, Cité Universitaire, Québec, Canada G1K 7P4*

We report on the application of chaos control to the irregular motion of an electron under the combined influence of a Coulomb and a magnetic field, the so-called “diamagnetic Kepler problem” (DKP). We show how to stabilize the classical chaotic orbits into regular motion and present a new method to follow the unstable orbits as the energy is increased from the regular to the chaotic regime.

PACS numbers: 05.45-a, 05.45.Gg

The dynamics of an hydrogen atom in a strong magnetic field is known as the “diamagnetic Kepler problem” (DKP). After more than two decades of research, the DKP is currently the most intensively studied autonomous, classically chaotic, atomic physics system. As first realized by Edmonds [1], the DKP is important in such diverse areas as solid state physics, astrophysics, and Rydberg atoms and occupies central stage in classical and quantum chaos research [2]. The classical flow covers a wide range of Hamiltonian dynamics reaching from bound, nearly integrable behavior to completely chaotic and unbound motion as the scaled energy is varied [3]. This letter reports the numerical implementation of a control scheme to stabilize this chaotic behavior. The methodology is sufficiently general to apply to *all* Hamiltonian flows and, with slight modifications, is also applicable to ballistic dynamics (e.g. billiards) and area-preserving mappings.

Ever since Ott, Grebogi and York (OGY) [4] introduced the notion of chaos control a decade ago, the number of experimental verifications has continuously and rapidly expanded to include a wide variety of applications ranging from magnetoelastic ribbons [5], electronic circuits [6], lasers [7], chemical reactions [8] to thermal convection loops [9]. The OGY algorithm was written explicitly for dissipative systems and most studies (experimental and theoretical) have focused their attention on this class of systems. Non-trivial modifications are needed to adapt the OGY technique to conservative flows (or maps) and Lai, Ding and Grebogi [10] have provided the necessary changes in the context of area-preserving mappings.

Our system is a continuous, 2 degrees of freedom (4D phase space) Hamiltonian flow representing the motion of an electron under the combined influence of a Coulomb and an external magnetic field. We use scaled semi-parabolic coordinates and write the resulting scaled (pseudo-) Hamiltonian as (for angular momentum  $L = 0$ )

[11]

$$\hat{h}_{DK} = \frac{1}{2}(p_\nu^2 + p_\mu^2) - \epsilon(\nu^2 + \mu^2) + \frac{1}{8}\nu^2\mu^2(\nu^2 + \mu^2) \equiv 2 \quad (1)$$

The scaled energy  $\epsilon$  is related to the physical energy  $E$  by  $\epsilon = \gamma_0^{-2/3} E$  where the parameter  $\gamma_0 = B/B_0$  denotes the strength of the magnetic field relative to the unit  $B_0 \simeq 2.35 \cdot 10^5 T$ . The structure of the dynamics of the Hamiltonian (1) depends solely on the value of the scaled energy  $\epsilon$ . For instance, it is known that for  $-0.5 < \epsilon < -0.13$  the system exhibits bounded motion with mixed chaotic and regular motion and for  $-0.13 < \epsilon < 0.0$  the last large stable island disappears and the dynamics is mostly chaotic [12].

The dimension reduction (from 4D to 2D) and discretization is performed by observing the dynamics on the Poincaré section defined by  $\mu = 0, \dot{\mu} > 0$ . The energy shell is then mapped to an area bounded by the condition  $p_\nu^2 - 2\epsilon\nu^2 = 4$  which represents an ellipse in the  $(\nu, p_\nu)$  plane. Figure (1) shows the collection of points  $\{\nu_n, p_{\nu,n}\}$  obtained by numerical integration of the equations of motion for  $\epsilon = -0.5$ . One notices, for this energy, that the *mixed* phase space is still mostly regular with a small stochastic area filled by the successive piercings of *one* chaotic trajectory. We recall that a periodic trajectory would show up on the Poincaré section as a finite number of crossings.

In attempting to bring order to the DKP dynamics, we had to overcome a number of difficulties not encountered in previous studies. We had in mind the *adaptive* control of chaotic DKP trajectories under changing conditions (e.g. drift in the magnetic field) through the stabilization of preselected unstable periodic orbits (UPOs) (monitored on the Poincaré section) via *small* programmed perturbations to the scaled energy. The difficulties are five-fold. First, a typical trajectory spends a lot of time away from the Poincaré section where the flow is discretized and because of the sensitivity of the chaotic dynamics we had to devise an efficient variable step *symplectic* integrator thereby preserving the geometrical structure of the Hamiltonian [13]. Second, the locations of a number of UPOs (our target states) and the corresponding Jacobian matrices for each member of the periodic orbits must be obtained numerically. It was found necessary to intervene at *every* crossing of the Poincaré section to assure a robust stabilization. Third, because of anomalous transport in Hamiltonian phase space [14], the waiting time

for a trajectory to enter the neighborhood of a predefined target UPO is unduly long and a *targeting* strategy is in general necessary to steer the trajectory towards the appropriate region of phase space. This problem has been addressed in [15] and is assumed to be solved. Fourth, the eigenvalues of area-preserving Jacobians are often complex and the stable and unstable manifolds, at the core of the OGY procedure, are no longer along the directions of their eigenvectors. A new method had to be implemented along the lines described in [10]. Fifth, a *tracking* algorithm for updating the control parameters (positions of UPOs, Jacobian matrices ...) was designed to insure that control is kept while external conditions are changing. Part of our solutions to these problems are discussed below and the details will be reported elsewhere.

To locate the UPOs on the Poincaré section, we have used two methods: a modified recurrence method (MRM) and an extension to conservative mappings of a stability transform algorithm (STA) introduced in [16]. The MRM uses the basic idea proposed by Auerbach *et al.* [17] for extracting periodic orbits from a chaotic time series  $\{\mathbf{X}_i\}_{i=1,N}$ . However, instead of scanning a very long  $N \gg 1$  time series for pairs of points separated in time by  $m$  iterates (for a period- $m$  UPO) and within a preassigned spatial distance  $r$  from each other,  $M$  points are launched on the Poincaré section and integrated forward until the  $m$ -th return on the section where the pair of points are compared. In both methods, the accepted pairs, a distance  $r$  apart, are distributed among the possibly different UPO candidates, the center of mass of each subset is calculated and the coordinates are stored. For a given relative accuracy,  $10^{-4} - 10^{-6}$ , we find  $M \ll N$  by several orders of magnitude. In Hamiltonian cases,  $N$  must be at least  $10^6$  in order to reach an acceptable precision. In the MRM, one can also easily take advantage of the symmetries on the Poincaré section for the flow. For example, figure (1) shows that the mapping is symmetric with respect to both  $\nu$  and  $p_\nu$  axes. Therefore one only needs to spread the initial conditions over one quarter of phase space for a smaller set of initial conditions or a denser distribution. This optimization is essential if one considers that between every two consecutive points on the Poincaré section, a segment of trajectory in phase space must be integrated numerically. Furthermore, for the DKP, this segment grows rapidly as the scaled energy approaches zero where the trajectory spends an increasingly long time in the branches (they grow as  $|\epsilon|^{-1/2}$ ) of the pseudo-potential.

The STA amounts to the following. Consider a discrete chaotic dynamical system  $S$  defined in a  $d$ -dimensional space by

$$\mathbf{X}_{n+1} = \mathbf{F}(\mathbf{X}_n, p) \quad (2)$$

where  $p$  is some external parameter. The goal is to construct from equation (2) other dynamical systems  $S_k$  with

the *same* periodic orbits (in number and positions), but whose stability has changed, i.e. unstable orbits become stable, and stable orbits remain stable. The new systems are defined by the linear transformations (written for a period  $m$  point,  $\mathbf{F}^{(m)}(\mathbf{X}^*, p) = \mathbf{X}^*$ )

$$\mathbf{X}_{n+1} = \mathbf{X}_n + \lambda \mathbf{C}_k [\mathbf{F}^{(m)}(\mathbf{X}_n, p) - \mathbf{X}_n] \quad (3)$$

where  $0 < \lambda \ll 1$  is adjusted to improve convergence and  $\mathbf{C}_k$  are non-singular constant  $d \times d$  matrices (see [16] for their explicit forms). Because of the stability of the periodic orbits of the constructed system  $S_k$ , every trajectory of  $S_k$  converges after a finite number of iterations to a periodic  $m$  point  $\mathbf{X}^*$ . Per construction, the  $\mathbf{X}^*$  are also periodic points of the original system  $S$ . We have tested this procedure for a number of area preserving mappings and flows and the global convergence of the method is excellent. For flows, where the mapping in (3) is replaced by a numerical integration for  $m$  returns to the Poincaré section, the STA has proved equally reliable. In this respect, our adaptive symplectic integrator [13] has insured that the (long) trajectories away from the Poincaré section were kept sufficiently accurate. The position of the fixed point in figure (2) (bottom panel) has been reached after only 250 iterations starting from an arbitrary initial point: this is representative of the efficiency of the STA. For the same relative accuracy ( $10^{-6}$ ), the MRM needs approximately  $10^4$  initial points.

In order to stabilize a chaotic trajectory around one of these UPOs, we have implemented a numerical version of the OGY method as modified in [10] for area-preserving mappings. This method is believed to be dynamically optimal in that it explicitly uses the local geometry of the underlying system. Given a dynamical system of the type (2), and a target UPO of period  $m$ ,  $\{\mathbf{X}(i, p_0)\}_{i=1,m}$ , at some nominal parameter value  $p_0$ , one characterizes the local stable and unstable manifolds by the vectors  $\mathbf{e}_{s,i}$  and  $\mathbf{e}_{u,i}$  respectively as well as their contravariant counterparts  $\mathbf{f}_{s,i}$  and  $\mathbf{f}_{u,i}$  satisfying  $\mathbf{f}_{u,i} \cdot \mathbf{e}_{u,i} = \mathbf{f}_{s,i} \cdot \mathbf{e}_{s,i} = 1$  and  $\mathbf{f}_{u,i} \cdot \mathbf{e}_{s,i} = \mathbf{f}_{s,i} \cdot \mathbf{e}_{u,i} = 0$ . The stabilizing perturbations  $\delta p_n \equiv p_n - p_0$  are then obtained by firstly linearizing the dynamics in a  $\delta$ -neighborhood of a member of the periodic orbit, say  $\mathbf{X}(k, p_0)$ , and around  $p_0$ , namely

$$\mathbf{X}_{n+1} - \mathbf{X}(k+1, p_n) \sim \mathbf{U}_k [\mathbf{X}_n - \mathbf{X}(k, p_n)] \quad (4)$$

where the  $d \times d$  Jacobian matrix  $\mathbf{U} \equiv D_{\mathbf{X}} \mathbf{F}(\mathbf{X}, p)$  is evaluated at  $[\mathbf{X} = \mathbf{X}(k, p_0), p = p_0]$  and it is understood that  $\|\mathbf{X}_n - \mathbf{X}(k, p_0)\| \leq \delta \ll 1$  and  $|\delta p_n| \ll |p_0|$ .

Secondly, the control criterion is imposed that  $\mathbf{X}_{n+1} = \mathbf{F}(\mathbf{X}_n, p_n)$  should lie along the *stable direction* at  $\mathbf{X}(k+1, p_0)$ , i.e.  $\mathbf{f}_{u,k+1} \cdot [\mathbf{X}_{n+1} - \mathbf{X}(k+1, p_0)] = 0$  which, together with the parametric variation of the periodic points,  $\mathbf{X}(k, p_0 + \delta p) \sim \mathbf{X}(k, p_0) + \mathbf{g}_k \delta p$ , leads to the following expression for the parameter perturbation at the  $n$ -th iteration:

$$\delta p_n = - \frac{\mathbf{f}_{u,k+1} \cdot \{\mathbf{U}_k [\mathbf{X}_n - \mathbf{X}(k, p_0)]\}}{\mathbf{f}_{u,k+1} \cdot (\mathbf{g}_{k+1} - \mathbf{U}_k \mathbf{g}_k)} . \quad (5)$$

The individual Jacobian matrices  $\mathbf{U}_i$  were obtained by least-square minimization [18] of the linear relationship between subsequent pairs of iterates on the Poincaré section for over 1000 points drawn from the close neighborhood of each  $\mathbf{X}(i, p_0)$ . For the dissipative cases, the eigenvectors of the Jacobian matrix  $\mathbf{U}_k^{(m)} = D_{\mathbf{X}}\mathbf{F}^{(m)}(\mathbf{X}_k, p_0) = \prod_{j=0}^{m-1} \mathbf{U}_{k+j}$  would determine the manifold directions, but as first realized in [10], the conservative cases lead generically to complex eigenvalues and eigenvectors and a different strategy is required. The solution adopted to generate the unstable (stable) direction  $\mathbf{e}_u$  ( $\mathbf{e}_s$ ) is to rotate an arbitrary unit vector  $\mathbf{u}_0$  ( $\mathbf{s}_0$ ) according to  $\mathbf{U}_k^{(qm)} \mathbf{u}_0$  and  $\mathbf{U}_k^{(-qm)} \mathbf{s}_0$  which converge respectively to  $\mathbf{e}_{u,k}$  and  $\mathbf{e}_{s,k}$  for  $q \gg 1$ . The vectors are periodically renormalized to prevent overflow and in general,  $q \leq 10$  is sufficient for convergence. This procedure is very reliable and robust.

Putting all the ingredients together, we have achieved the stabilization of the chaotic behavior of the diamagnetic-Kepler Hamiltonian (1) for different values of  $\epsilon$  and different UPOs. Figure (2) presents a sample of results for the control of period-2, period-3 and period-1 at  $\epsilon = -0.3, -0.2$  and  $-0.1$  respectively. The control mechanism was switched on when an iterate entered a neighborhood of size  $\delta = 10^{-3}$  ( in the 3 panels, one has removed the initial transient) and the perturbations on the scaled energy (alternatively the magnetic field) were never larger than  $\delta\epsilon = 10^{-2}$ . After 3000 iterates, we release the control,  $\delta\epsilon_n = 0$ , and the trajectory returns to its natural chaotic behavior. One also notes (left panels) that the dynamics is increasingly chaotic as  $\epsilon$  approaches zero and by  $\epsilon = -0.1$  no obvious trace of regularity is present. We emphasize that in performing the present control task no *a priori knowledge* of the governing map on the Poincaré section is known and the complete procedure is purely numerical from beginning to end.

Under parameter variation, the location of the UPOs changes as well as their associated Jacobian matrices, and unless action is taken the control over the chaotic dynamics may be lost. The strategy of detecting parameter drift and updating accordingly the control parameters is known as *tracking* [19]. We have developed a new tracking algorithm which is simple and efficient. For concreteness, we will concentrate the presentation on the updating localization of the UPOs.

The method is based on a judicious construction of a family of *extrapolating rational functions* [20]. One starts from a number  $s$  of UPO coordinates (the seeds), e.g.  $\{\nu_i, \epsilon_i\}_{i=1,s}$ , from which a rational function,  $R_0(s, \epsilon)$  is constructed.  $R_0$  is then evaluate at  $\epsilon_{s+1} = \epsilon_s + \Delta\epsilon$  with  $\Delta\epsilon \ll 1$  to give an extrapolated value  $\nu_{s+1}$ . A new set of seeds is formed  $\{\nu_{i+1}, \epsilon_{i+1}\}_{i=1,s}$ , removing  $\{\nu_1, \epsilon_1\}$  and keeping the number of seeds fixed, and a new ex-

trapolating function  $R_1(s, \epsilon)$  is calculated. The process is repeated until a final value  $\epsilon_f$  is reached. The same procedure may also be applied to the pairs  $\{p_{\nu,i}, \epsilon_i\}_{i=1,s}$  to provide initial conditions  $\{\nu_i, p_{\nu,i}\}$  for the integration of the complete phase-space trajectory. Two remarks are in order. First, this approach is much more accurate at  $\epsilon_f$  than the direct extrapolation  $R_0(s, \epsilon_f)$ , although all the original seeds are replaced by extrapolated values after  $s$  iterations. Second, the algorithm permits to cover a wide range of parameter variations beyond the initial seeds (3-5 in practice) while keeping high accuracy. Since the individual extrapolation steps are chosen small, we call the method *adiabatic localization* (AL) or more generally *adiabatic tracking* (AT).

We have applied AT to the dissipative Hénon map for the same range chosen in [19]. The results are in complete agreement with those of [19] and with the precise values of the position of UPOs obtained by STA. We have also applied this algorithm to the standard map, the Hénon-Heiles Hamiltonian and the DKP and more complete results will be reported at a later time. Figure (3) shows the tracking of a period-1 orbit for the DKP. We started from five seeds for  $\epsilon$ : - 0.3, - 0.29, - 0.28, -0.27, -0.26 and set  $\Delta\epsilon = 0.001$ . The tracking process is extended to  $\epsilon = -0.075$ . The results from the STA confirms the accuracy of the adiabatic tracking. The right panel clearly indicates that the result from AT for  $\epsilon = -0.075$  is indeed a period 1 orbit.

We have presented for the first time the application of a numerical implementation of the OGY control to a realistic conservative flow, the DKP Hamiltonian. On our way to a complete solution, we have i. developed a new variable step symplectic integrator, ii. modified the standard recurrence method and extended a powerful technique (STA) to locate the positions of the unstable periodic orbits, iii. obtained accurate numerical Jacobian matrices and the local manifolds, and iv. provided an efficient approach (AT) for tracking the UPOs under parameter changes. We are presently considering two important mesoscopic applications: nonlinear dynamics in electromagnetic traps [21], and chaotic ray dynamics in lasing microcavities [22]. It still remains an open question however if manipulations of an external parameter (e.g. a magnetic field) to induce stabilization of a classical unstable orbit can be extended to the semi-classical regime, for example, for the control of Rydberg wave packet dynamics. Research along these lines is actively being pursued.

---

\* Corresponding author. E-mail: ljd@phy.ulaval.ca  
[1] A. R. Edmonds, *J. Phys. B* **6**, 1603 (1973).

- [2] R. Blümel and W. P. Reinhardt, *Chaos in Atomic Physics* (Cambridge University, Cambridge, 1997).
- [3] J. B. Delos, S. K. Knudson, and D. W. Noid, *Phys. Rev. A* **30**, 1209 (1984)
- [4] E. Ott, C. Grebogi, and J. A. Yorke, *Phys. Rev. Lett.* **64**, 1196 (1990).
- [5] W. L. Ditto, S. N. Rauseo, and M. L. Spano, *Phys. Rev. Lett.* **65**, 3211 (1990).
- [6] E. R. Hunt, *Phys. Rev. Lett.* **67**, 1953 (1991).
- [7] R. Roy, T. W. Murphy Jr., T. D. Maier, and Z. Gills, *Phys. Rev. Lett.* **68**, 1259 (1992).
- [8] V. Petrov, V. Gáspár, J. Masere, and K. Showalter, *Nature* (London) **361**, 240 (1993).
- [9] J. Singer, Y. Z. Wang, and H. H. Bau, *Phys. Rev. Lett.* **66**, 1123 (1991).
- [10] Y. C. Lai, M. Ding, and C. Grebogi, *Phys. Rev. E* **47**, 86 (1993).
- [11] H. Friedrich and D. Wintgen, *Phys. Rep.* **183**, 37 (1989).
- [12] G. Tanner, K. T. Hansen, and J. Main, *Nonlinearity* **9**, 1641 (1996).
- [13] R. Poulin, B. Pourbohloul, and L. J. Dubé (in preparation).
- [14] J. D. Meiss, *Rev. Mod. Phys.* **64**, 795 (1992).
- [15] E. M. Bollt and J. D. Meiss, *Physica D* **81**, 280 (1995); C. G. Schroer and E. Ott, *Chaos* **7**, 512 (1997).
- [16] P. Schmelcher and F. K. Diakonov, *Phys. Rev. Lett.* **78**, 4733 (1997); *Phys. Rev. E* **57**, 2739 (1998).
- [17] D. Auerbach, P. Cvitanovic, J.-P. Eckmann, G. Gunaratne, and I. Procaccia, *Phys. Rev. Lett.* **58**, 2387 (1987).
- [18] J. P. Eckmann, S. O. Kamphorst, D. Ruelle, and S. Ciliberto, *Phys. Rev. A* **34**, 4971 (1986); M. Sano and Y. Sawada, *Phys. Rev. Lett.* **55**, 1082 (1985).
- [19] T. L. Carroll, I. Triandaf, I. Schwartz, and L. Pecora, *Phys. Rev. A* **46**, 6189 (1992); I. B. Schwartz, T. W. Carr, and I. Triandaf, *Chaos* **7**, 664 (1997).
- [20] W. H. Press, S. A. Teukolsky, W. T. Vetterling, and B. P. Flannery, *Numerical Recipes in C, 2<sup>nd</sup> ed.* (Cambridge University Press, Cambridge, 1992).
- [21] W. Paul, *Rev. Mod. Phys.* **62**, 531 (1990).
- [22] J. U. Nöckel and A. D. Stone, *Nature* (London) **385**, 45 (1997).

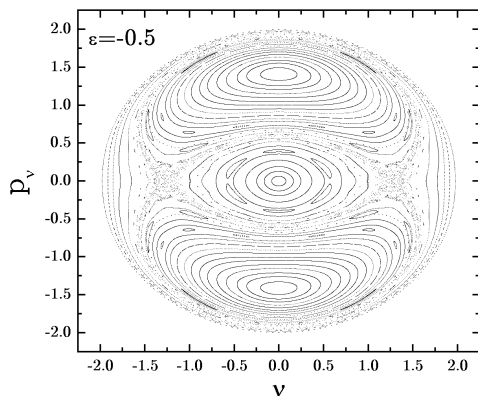


FIG. 1. Poincaré section of the DKP for  $\epsilon = -0.5$ .

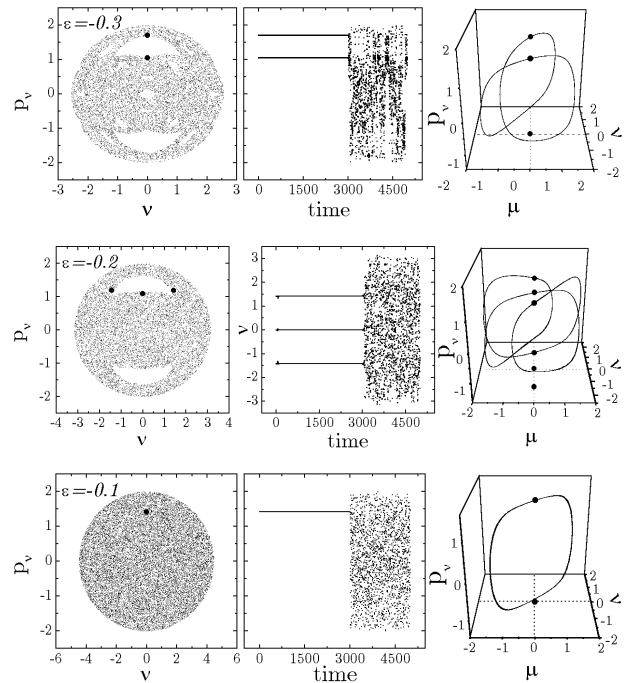


FIG. 2. OGY Control of Diamagnetic Kepler orbits for 3 scaled energies  $\epsilon_0 = -0.3, -0.2, -0.1$  and periods 2, 3, 1 in top, middle, and bottom panels: (left) Poincaré section (PS)  $\mu = 0, \dot{\mu} > 0$  showing one chaotic trajectory (filled space) and the controlled UPO (black dots); (middle) the stabilized  $p_\nu$  or  $\nu$  variable for the first 3000 intersections with the PS before control is turned off; (right) corresponding 3D stabilized trajectory.

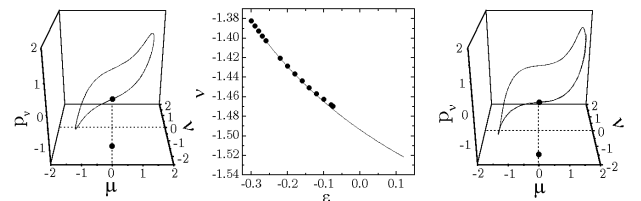


FIG. 3. (middle) Tracking of an unstable fixed point for  $-0.3 \leq \epsilon \leq -0.075$ . Solid line: AT.  $\bullet$ : STA. (left) 3D trajectory for  $\epsilon = -0.3$ . (right) 3D trajectory for  $\epsilon = -0.075$ . The initial condition for this trajectory is that obtained by adiabatic tracking, i.e. ( $\nu^* = -1.46942$ ,  $p_\nu^* = -0.000133596$ ).